Designing Evacuation Routes Considering Risk and Clearance Times

Daniel Rivera-Royero
Institute of Transportation Studies
University of California
One Shields Ave, Ghausi Hall, Room 2001
Davis, CA, 95616
Email: riveraroyero@ucdavis.edu

Miguel Jaller, Corresponding Author
Department of Civil and Environmental Engineering
Sustainable Freight Research Program
Institute of Transportation Studies
University of California
One Shields Ave, Ghausi Hall, Room 3143
Davis, CA, 95616
Email: mjaller@ucdavis.edu

Submitted August 1st , 2024

Word Count: 7,500

ABSTRACT

This paper introduces a method for designing evacuation plans considering wildfire risks to minimize clearance time and the resources used, e.g. road network corridors. The study considers wildfire risks resulting from historical event information, populations' social vulnerability, and the road network's topological characteristics. The methodology combines mathematical programming optimization models and risk assessment. The main data sources include OpenStreetMap (OSM), the American Community Survey (ACS), and the National Risk Index (NRI). Furthermore, the study uses fire projections from a specific case study to evaluate evacuation performance. The methodology estimates the clearance time for evacuation, measures the risk perceived by evacuees from potential wildfires, and evaluates the expected efficiency of the evacuation during different scenarios, including a real-life wildfire event. Our results demonstrate the need to identify alternative or supportive strategies to evacuation in scenarios of no or short notice when a city's current capacity cannot effectively manage evacuation during a wildfire.

Keywords*:* Evacuation, Optimization, Wildfires, Road Network Performance

INTRODUCTION

Natural hazards are all those extreme weather and geophysical events with the potential to threaten human safety and health, critical infrastructure, property, and homeland security. Natural hazards include floods, tornadoes, winter storms, hurricanes, wildfires, and earthquakes [1]. The socioeconomic consequences of natural hazards vary significantly depending on the type of hazard and the impacted location [2]. Wildfires are a major concern in the wildland-urban interface areas (WUI), where people live surrounded by wildfire-driven fuels [3].

Between 2017 and 2019, eleven large-scale wildfires caused the evacuation of at least ten thousand individuals [4] in California. Evacuation involves the movement of people at risk to safer places at minimal risk [5]. Heavy congestion is a common factor when dealing with urban evacuation that relies on road networks because the influx of vehicles can quickly saturate the limited exit routes [5]. Road network functionality is essential for safe evacuations and enabling disaster response operators to reach the population adequately [6]. In the US, 2018 was the year with the highest cost on property damage, business interruptions, and agricultural losses due to wildfires, with $30bn, followed by 2017 and 2020, with $23bn and $20bn, respectively [7].

Additionally, the 2018 Camp Fire is known as California's deadliest and most destructive wildfire in the last 90 years of wildfire records, with 85 fatalities and 18,804 structures destroyed [8]. One of the reasons for such devastating consequences is that it was a fast-moving wildfire, where many vehicles attempted to escape on a restricted road network with short notice. Based on Blanchi et al. [9], early evacuation is the preferred disaster management strategy during wildfires in the US. However, on certain occasions, anticipated evacuations are impossible due to the information about the wildfire being available at short or no-notice time, resulting in catastrophic consequences as occurred in the 2018 Camp Fire.

In the literature, evacuation risk is usually assessed using surveys [10] or by assessing the time when the natural hazard would hit a particular asset of the road network [11]. However, applying the results of a local survey to other locations with different contexts and population characteristics may be challenging. This is critical under a short- or no-notice wildfire because it is practically impossible in such a situation as it is already too late to assess the risk. Therefore, anticipating the expected wildfire risk for evacuation purposes in a generalizable manner allows planners to design evacuation plans (e.g., design evacuation routes, mitigate risks in those routes, adapt the infrastructure, and identify safe locations) for different locations.

This paper aims to design wildfire evacuation plans based on anticipated risk measurements. Such evacuation plans enable the identification of the most critical corridors (arcs/links) within a road network, which are essential for the evacuation process. The study estimates an evacuation risk based on wildfire historical information, social vulnerability determined by the socioeconomic characteristics of the population, road network topology, and evacuation route utilization. The importance of the corridor lies in its robustness and polyfunctionality under different scenarios. Identifying these corridors will permit planners to prioritize investments or attention to enhance their resilience against natural hazards, particularly those that require evacuations. Finally, the authors plan to evaluate the performance of the evacuation plan against a simulated wildfire event where evacuation is critical.

LITERATURE REVIEW

Disaster operation management (DOM) includes the activities performed before, during, and after a natural or anthropogenic disaster [12]. DOM activities have the potential to diminish the impact of those events and contend with numerous uncertainties that increase their complexity, e.g., unknown demand and supply, disrupted information systems, shorter response times, and social impacts [13]. DOM strategies include mitigation, preparedness, response, and recovery [14]. Commonly, DOM relies on operations research and management science (OR/MS) [15]. For instance, applications for prepositioning supplies [16], distributing relief items [17], and evacuation are among the most important DOM strategies to save lives before/during natural hazards such as hurricanes, wildfires, and tsunamis.

The evacuation process depends on the natural hazard. For instance, hurricane evacuations affect a larger land area and more people than wildfire evacuations. Additionally, the distance between the affected

area and safe destinations is larger in hurricanes than in wildfires. US disaster managers prefer an early evacuation process in case of wildfires [18]; however, it is not always possible. For example, evacuation activities cannot be done in advance when a short- or no-notice wildfire occurs. This makes evacuations more complex than when early evacuation is possible [19].

In the literature, researchers study evacuation by considering behavioral and engineering perspectives. From the first perspective, researchers try to distinguish the factors that influence the decisions of the evacuees. Including behavioral elements in the transportation models allows a more realistic estimation of the evacuation time [20, 21]. Studies draw inferences on behaviors from surveys of the affected population after specific disasters or by stated preference surveys evaluating hypothetical scenarios. This method provides valuable information but lacks a straightforward generalization to other areas and situations. However, some authors assume that such generalization is possible and use it in their models [19].

From the engineering perspective, researchers focus on time performance estimation and traffic flow modeling, among others [20]. The strategies to deal with evacuations from the engineering perspective can be on the demand and supply sides of the transportation network. Strategies for the traffic supply include transit operations, special signal timings, shoulder lane use, crossing elimination, and contraflow operations [22, 23, 19]. The demand side includes evacuation staging, departure time, route assignment, and reducing shadow or background traffic [23, 22].

This paper analyzes the performance of evacuation plans through optimization models, considering expected wildfire risk, evacuation time, vehicle demand, and road network capacities. Note that the primary goal of this paper is to identify how the current state of the road network may affect evacuation performance and develop a generalized methodology for various locations. This scope limits the direct consideration of behavioral elements; however, the study considers the population's socioeconomic characteristics in the evacuation risk analysis estimation.

Figure 1 summarizes relevant evacuation studies from the perspective of the evaluation approaches: mathematical programming (MP) and simulation (S), with MP&S being the sub-set with the largest share. Among the papers belonging to MP, only [24], [25], and [26] analyze the evacuation without including *shelters* as an option. On the one hand, [24] uses a time-expanded model to optimize the evacuation plan, and [25] models the capacity-constrained evacuation scheduling problem over discrete time as an integer optimization model. These approaches suffer from high computational costs and do not scale to large transportation networks. On the other hand, [26] provides a method to obtain the optimal egress time and path generation for large evacuation networks when all the population is requested to evacuate with no predetermined priorities, obtaining a set of mathematical models able to handle large-size networks with low computation time. Among papers on the MP set, only [27] include a risk analysis based on the time exposed to a particular hazard.

Figure 1 Literature Review Summary

In the simulation set (S), [10] used a household survey to model the risk perception of wildfire in a traffic simulation model. This survey method works well for evacuees' behavior in the specific case of Mati, Greece; however, such results cannot be generalized to other cases in different places. [11] discuss

another type of risk assessment based on priorities determined by the time the natural hazard is expected to affect a given node, allowing only a limited time for the population in those nodes to evacuate. They implement the method in a hurricane setting with path projections made in advance. In the event of a short- or no-notice wildfire, such projections are not feasible, as the information is usually unavailable, and the evacuation should be performed quickly. Therefore, it is essential to use a methodology that is adaptable to different settings and does not depend on a priory projection but instead provides a robust plan for various situations, such as short- or no-time wildfire events.

The literature review highlights the need to develop a generalizable method to design evacuation plans based on risks. This method should incorporate general information from each location, such as historical wildfire data, socioeconomic characteristics of the population, and road network topology. One of the objectives of developing evacuation plans is identifying the most critical corridors within a road network examining various scenarios, including simulated real-life wildfires. Additionally, identify corridors' performance regarding time, risk, and resource minimization to enhance their resilience for vulnerable populations in future evacuations.

METHODOLOGY

The authors propose a five-stage modeling framework to design evacuation plans with a wildfire risk assessment depicted in Figure 2.

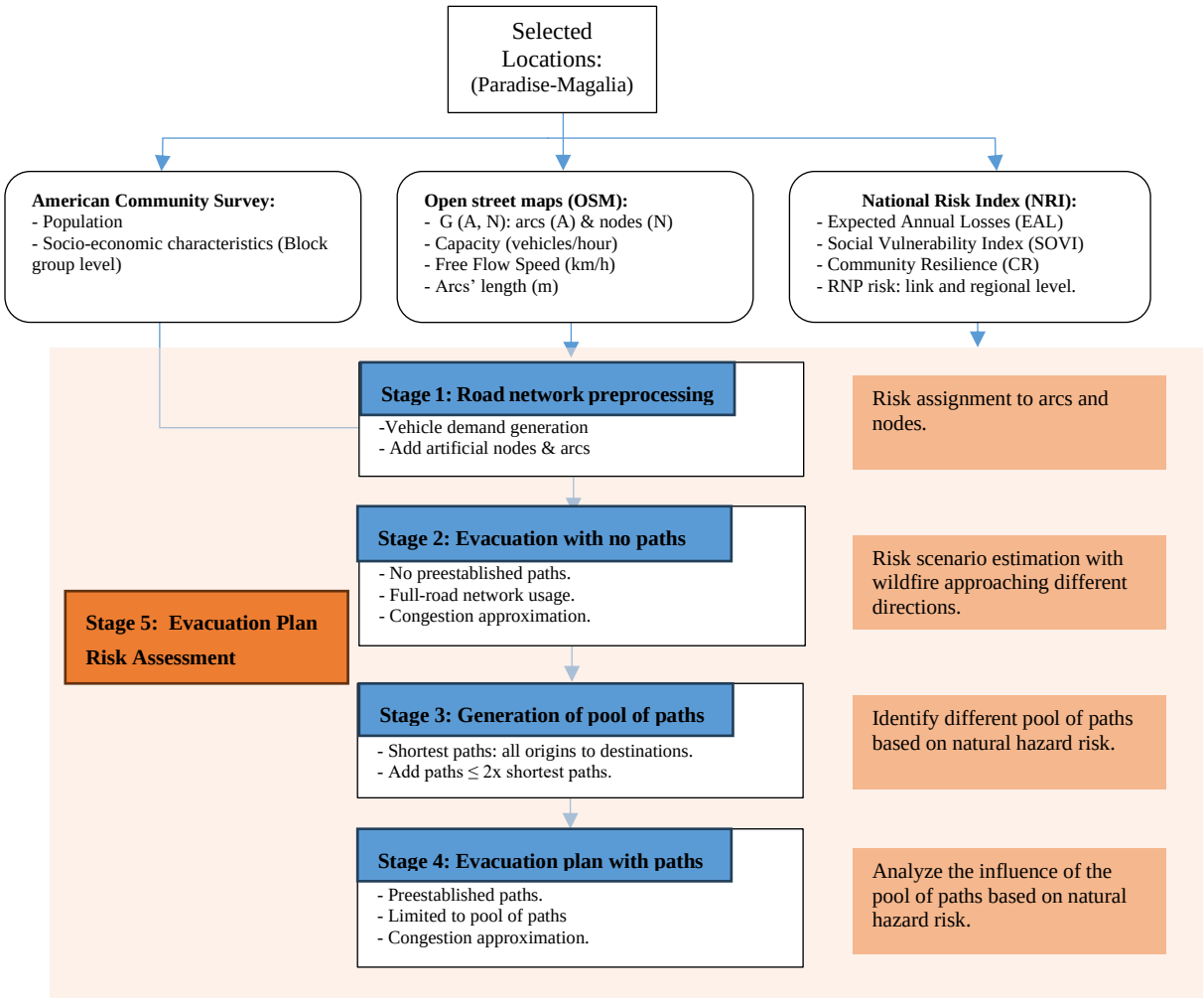

Figure 2 General methodology

Stage 1: Road network preprocessing

First, the authors used Open Street Maps (OSM) to obtain the road network $G = (N, A)$, where N is the set of nodes (or intersections) and A arcs (or streets) [28]. If required, complex intersections in road networks can be simplified to reduce the complexity of the mathematical models. The nodes N can be classified as intermediate (N_i) or sink (N_s) nodes. N_s are the nodes connected to external nodes that lead to safe destinations outside the road network. Additionally, the arcs obtained from OSM contain information about the highway type and length and partial information about the maximum speed and number of lanes. The mathematical models consider the arc's travel time (tt) and capacity (μ). To estimate the tt, the authors use the arc's length (l) and speed (v) ($tt = l/v$). To obtain the μ, and number of lanes and the speed for those arcs with not information available in OSM, the authors use the information described in [29] that depends on the highway type. To model the traffic demand, we create two types of artificial nodes: source nodes (N_a)) and a super-node (SN).

- **Source Nodes (N_a)**: These are origin nodes, with one N_a corresponding to each census block group (CBG) in the location. The vehicle demand assigned to each N_a can be obtained from the American Community Survey (ACS), by using the average households' size and vehicle availability per CBG [30]. N_a are connected to the road network via the two closest nodes using artificial arcs.
- **Super-Node (SN)**: This artificial node is connected to the all the N_s. SN has enough capacity to attract the total vehicle demand, simplifying the problem into a multiple origin and single destination problem. Let us remark that this model evacuates the population to external areas outside the network, and no internal safe locations were considered.

The artificial arcs connecting N_a to the road network and N_s to SN have zero travel time and high capacity, ensuring smooth flow.

This study builds on the methodologies discussed in [26] to develop the models in Stages 2, 3, and 4. The differences between our models in this paper and the models in [26] are described as follows:

Stage 2: Evacuation with no paths (ENP)

The problem setting in this stage is to evacuate all vehicle demand from N_a to a safe location outside the road network, the SN. In this case, there is no pre-established path; vehicles can use the entire road network and leave it as soon as possible without exceeding arcs' capacities. The mathematical formulation of the ENP model is in Figure 3.

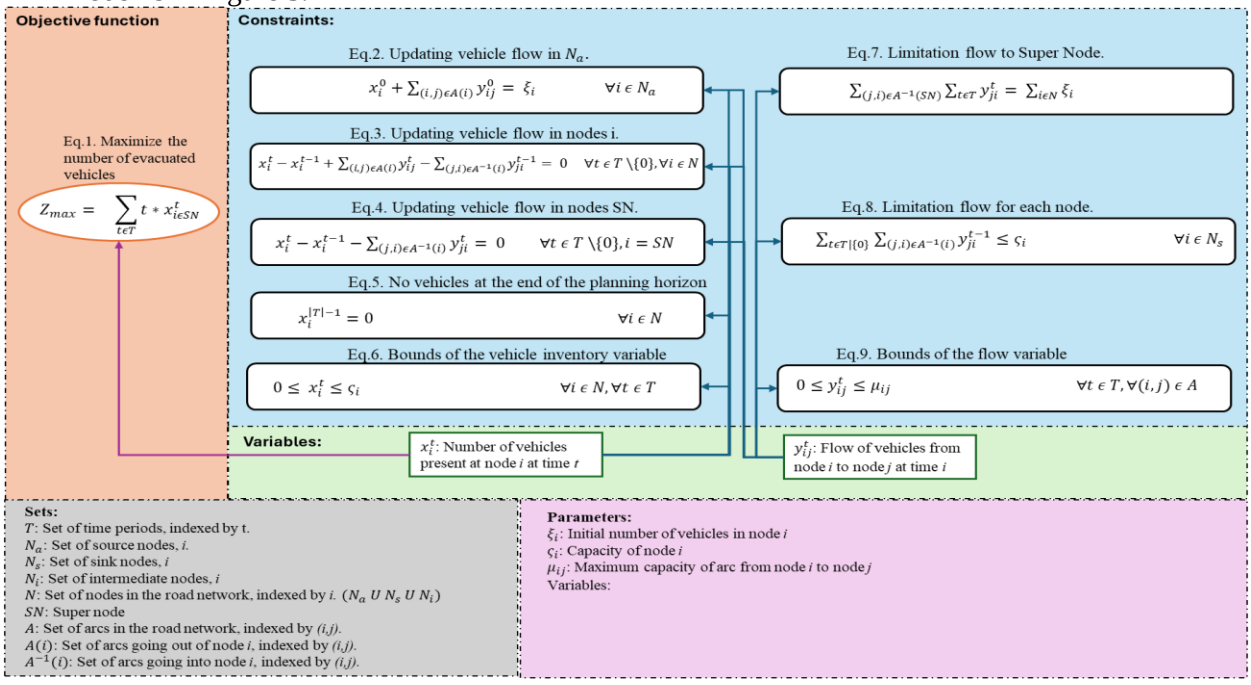

Figure 3 Evacuation with no paths (ENP) model

One of the main differences between the ENP and the Minimum Egress Time (MET) model described in [26] is in the objective function. The objective function of the ENP is to maximize the cumulative number of vehicles evacuated to the SN weighted by time ($Z_{max} \sum_{t\,\epsilon T} t * x^{t}_{i\epsilon SN}$) (see Eq.1), while the objective of the MET is to minimize the flow of vehicles to the N_s for each time-unit (TU) in the planning horizon ($Z_{min} \sum_{t\,\epsilon T} \sum_{(i,j)\epsilon A(N_s)} t * y^{t}_{(i,j)}$). In both cases, the objective is to minimize the time when all vehicles evacuate the location; however, Eq.1 avoids possible delays in the flow from N_s to the SN, as may occur in MET. The ENP model is designed for road networks with arcs with 1 TU travel time. Initially, travel times could be in seconds; therefore, converting those travel times into TUs is necessary. One TU is the value of the minimum travel time within all the arcs ($\min(tt_a)$), and the travel time for each arc in TU is obtained as $TU_a = \lceil \mathrm{tt_a} / \min(tt_a) \rceil$. After determining the travel time in TU units, it is necessary to add as many artificial nodes and arcs as required between each pair of nodes with travel times greater than one TU. For example, if the minimum travel time in free flow in the road network is 10 seconds, and the travel time for a random arc in free flow speed is 60 seconds, then it requires 6 TUs to cross the arc. Therefore, it is necessary to add 5 artificial nodes between these two nodes, connected by 6 arcs with one TU each and capacity transformed to the number of vehicles per $\min(tt_a)$. This process results with a road network with a larger size, $G_{mod} = (N_{mod}, A_{mod})$. From Figure 3, Eq.2 initializes the demand for vehicles to each N_a. Eq.3 is a flow balance constraint to each node. Eq.4 updates the number of vehicles reaching the SN by adding the flow entering the *SN* from all the N_s. Eq.5 establishes that at the end of the planning horizon, the road network is empty, while Eq.6 and Eq.9 provide the bounds and the integer nature of each decision variable. Note that in Eq.6, the ς_i for intermediate nodes N_i, must be zero, while for Eq.9, the arc's flow value is constrained by the arc's maximum capacity during each time. Eq.7 establishes that all the demand at the beginning of the planning horizon reaches the SN, and the time 't' when the total demand is evacuated is when Eq.7 is activated. Finally, Eq.8 restricts the flow entering the N_s to their capacities.

Stage 3: Generation of a pool of paths

The GPP model uses the original road network described in Stage 1, and the mathematical formulation is depicted in Figure 4.

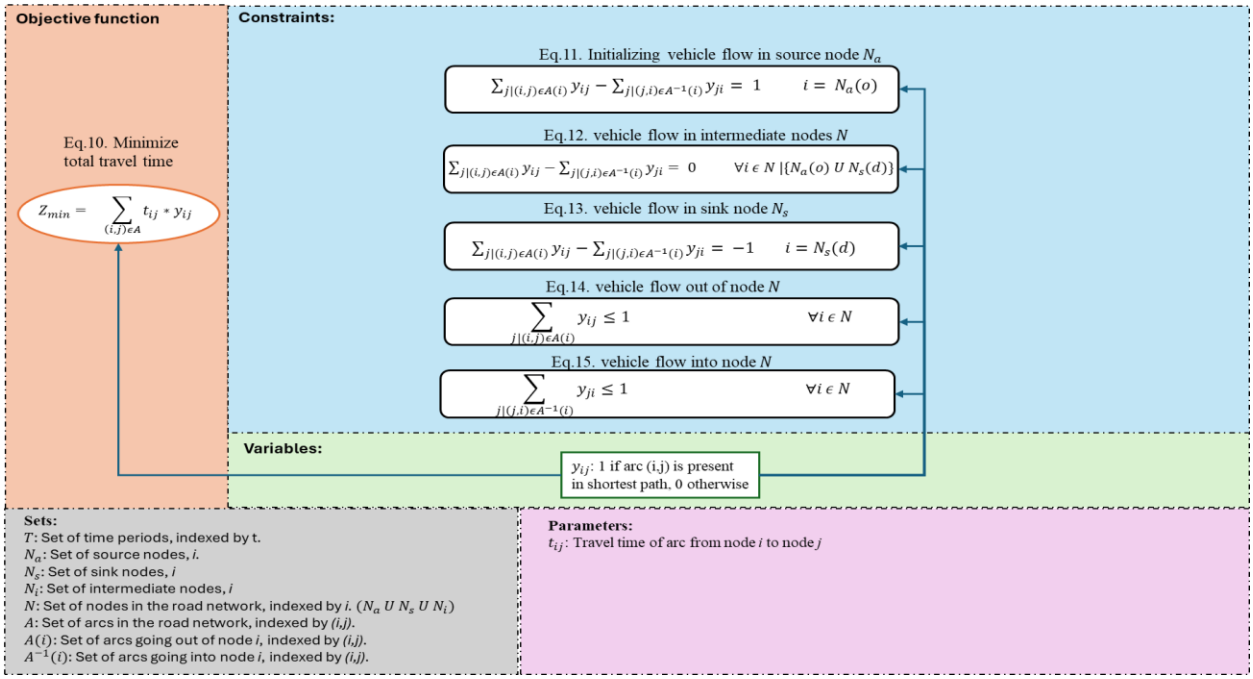

Figure 4 Generation of a pool of paths (GPP) model

The difference between the GPP and PG models, described in [26], is in the problem setting. The GPP model estimates the shortest path between each pair of nodes (N_a, N_s), instead of obtaining the shortest paths between each origin node N_a to the SN. The advantage of this assumption is that it creates a more diverse set of paths compared to the method implemented in [26]. The pool of feasible paths includes those with an objective function that can be, at most, double the optimal shortest path time for each Origin-Destination pair. In Eq.10, the authors seek to minimize the total travel time in the network for one origin and destination pair (N_a, N_s). Eq.11 indicates that from the selected origin node, only one arc exiting this node can have a non-zero value. Eq.12 indicates that the sum of the arcs selected to enter each node must be equal to the ones that exit (clear the system). Eq.13 indicates that only one arc must be selected to enter the sink node. Eq.14 and 15 provide the bounds of the decision variable.

Stage 4: Evacuation plan with paths

Figure 5 depicts the mathematical formulation of the EPWP model. The pool of paths obtained from Stage 3 is an input to the EPWP model, and the initial value of T is the clearance time (CT) obtained in Stage 2. Note that no feasible solution may be found when solving the EPWP with the CT and the pool of paths. Therefore, the EPWP is resolved iteratively, increasing the value of T by one unit for each iteration until the optimal solution is found.

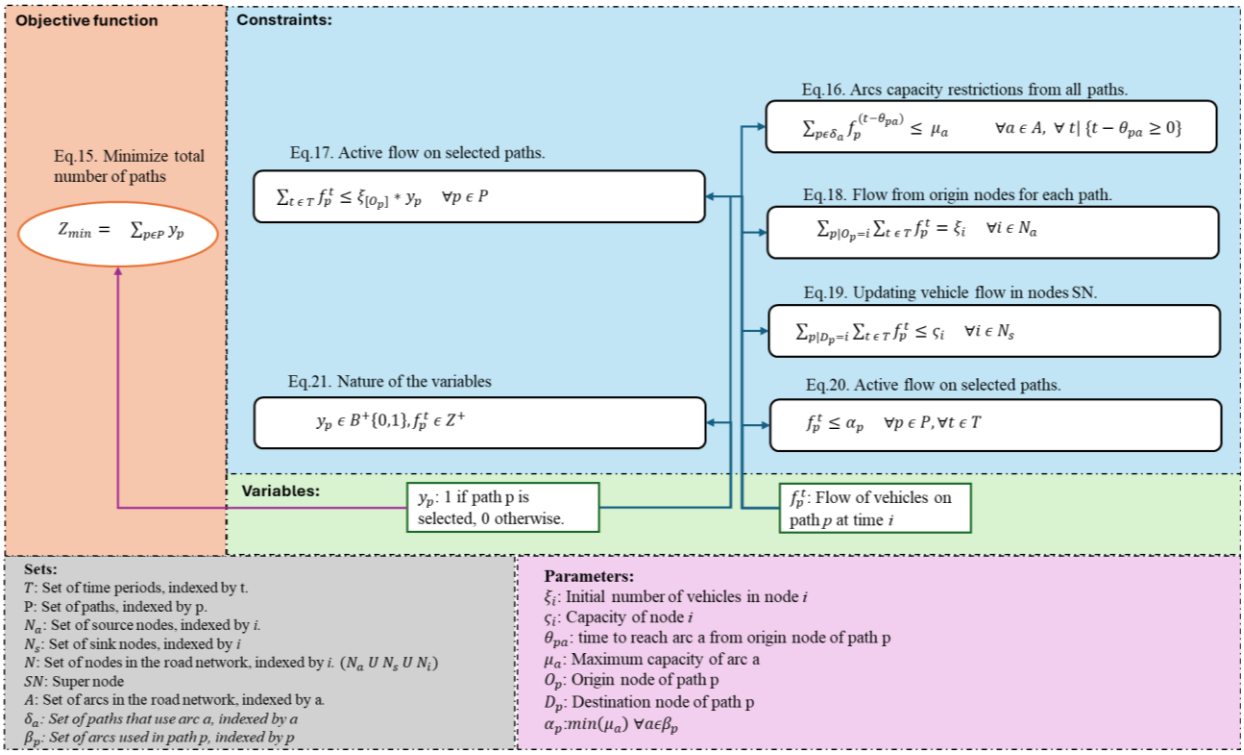

Figure 5 Evacuation plan with paths (EPWP)

Eq.15 seeks to minimize the number of selected paths for evacuation. Eq.16 ensures that the incoming flow from all the paths reaching the arc a at time $t - \theta_{pa}$ to be lower or equal to the maximum capacity of the arc. Eq.17 indicates that the total flow departing from path p if selected, should be lower or equal to the initial demand at the N_a. Eq.18 establishes that the total flow leaving each N_a must be equal to the initial vehicle demand. Eq.19 establishes that the total flow entering N_s cannot exceed its capacity. The main difference between the EPWP model and the PSFG described in [26] is the addition of Eq.20, where the flow departing from each path at any time during the planning horizon cannot exceed the maximum capacity of the arc with the minimum capacity belonging to each path. This constraint avoids possible overlapping flow in all the arcs. Finally, Eq.21 provides the nature of the decision variables.

Stage 5: Evacuation Plan Risk Assessment

A description of how risk assessment is performed in the four stages discussed before is as follows.

- ***Stage 1***: First, it is required to estimate the Road Network Risk (RNP^{z}_{risk}) for wildfires. For this, the authors follow the methodology developed in [31]. This methodology assesses the RNP_{risk} for different natural hazards (z) at three different levels of the road network: i) node level (v_i^z), ii) regional level (ψ_r^z), and iii) global level (Standardized Spatial Risk Index ($SSRI^z$)). In this paper, the authors use the risk at the node level (v_i^z), and at the regional level (ψ_r^z), but not the $SSRI^z$, specifically for wildfires. v_i^z depends on the road network's topology given by the Betweenness Centrality (BC_i) and the Hansen Accessibility Index (A_i) of each node. Additionally, v_i^z depends on the National Risk Index (NRI) (θ_i^z) defined at the node level [32]. NRI depends on the expected annual losses (EAL) from historical data of a set of different natural hazards, and its consequences increase when the Social Vulnerability index (SOVI) is high but are reduced when the Community Resilience (CR) is high. The SOVI and CR are two indexes that depend on the socioeconomic characteristics of the population living in the area. v_i^z formulation is given in Eq.22:

$$v_i^z = \frac{\theta_i^z * BC_i * A_i}{\sum_{j=1}^{n}\left(\theta_j^z * BC_j * A_j\right) - \theta_i^z * BC_i * A_i} \quad \text{Eq. 22}$$

- **Stage 2:** The function of ψ_r^z is to group the v_i^z based on the directions or regions R from the center of the road network and to obtain its average, as described in Eq.23. Note that R is the set of regions, ranging from 0 to 360 degrees in increments of 10 degrees, e.g., r= {0, 10, 20, …, 350}, and n_r is the number of nodes that belong to each region r.

$$\psi_r^z = \frac{1}{n_r}\sum_{i \in r} v_i^z \quad \forall r \in \text{R} \quad \text{Eq. 23}$$

ψ_r^z is used to estimate the likelihood of a wildfire in specific directions of the network and analyze the sensitivity of the evacuation process if different exit routes are closed due to wildfire.

- **Stages 3 and 4:** The authors identify how the population's socioeconomic characteristics affect the evacuees' perceived risk and evacuation time. The original objective function of the GPP model given in Eq.10 is travel time minimization from the origin node N_a to destination node N_s. To analyze how the evacuation pattern changes, the authors modified the GPP model's objective function to obtain different paths to use as input to the EPWP model. The two alternative objective functions are:

$$Z_{min} \quad \sum_{(i,j)\epsilon A} r_{ij} * y_{ij} \quad \text{Eq. 24}$$

$$Z_{min} \quad \sum_{(i,j)\epsilon A} t_{ij} * r_{ij} * y_{ij} \quad \text{Eq. 25}$$

Where Eq.24 minimizes the risk of the selected path, and Eq.25 minimizes the risk and time for each origin N_a to destination N_s. r_{ij} is the risk associated with the link (i, j), and it is obtained as the average of the v_i between each pair of nodes (See Eq.26).

$$r_{ij} = \frac{v_i + v_j}{2} \quad Eq. 26$$

EMPIRICAL RESULTS & DISCUSSION

The authors use the 2018 Camp Fire in Paradise and Magalia, California, as the case study in this work.

Stage 1: Road network preprocessing

Figure 6 shows the map of Paradise and Magalia, highlighting the sink (X) and origin (O) nodes. Each origin node has assigned a vehicle demand obtained from the American Community Survey at the Census Block group level. Additionally, Figure 7 summarizes the most important parameters from the 1860 arcs of the road network of Paradise and Magalia. The arc's length ranges from 101 to 2722 meters, and most arcs are shorter than 1 km (1000 m). Furthermore, the arc's capacity ranges from 600 to 4000 vehicles/hour, and most arcs have a capacity of 1200 vehicles/hour or less.

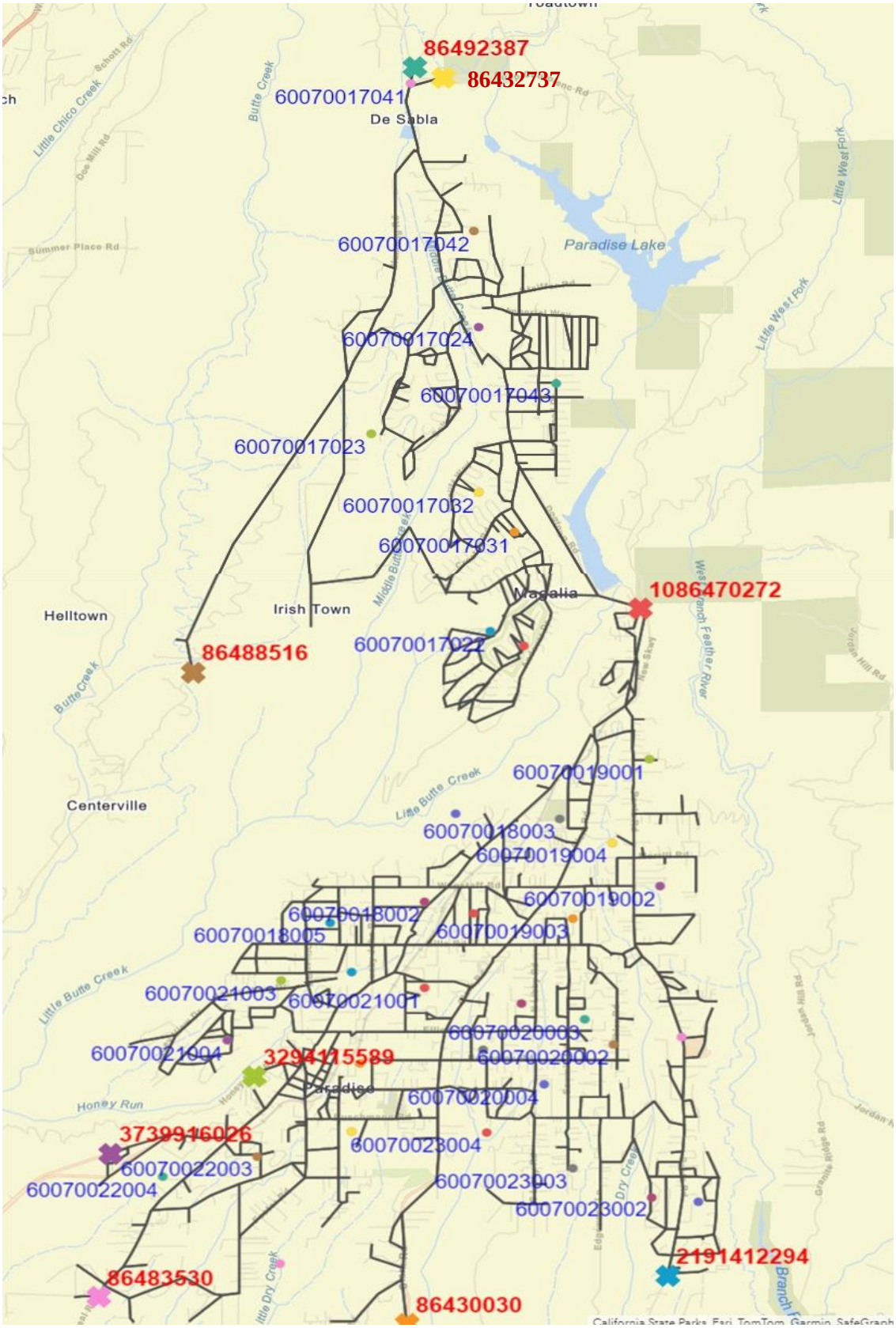

Figure 6 Paradise Map with the labels of the source and sink nodes demand and sink capacity

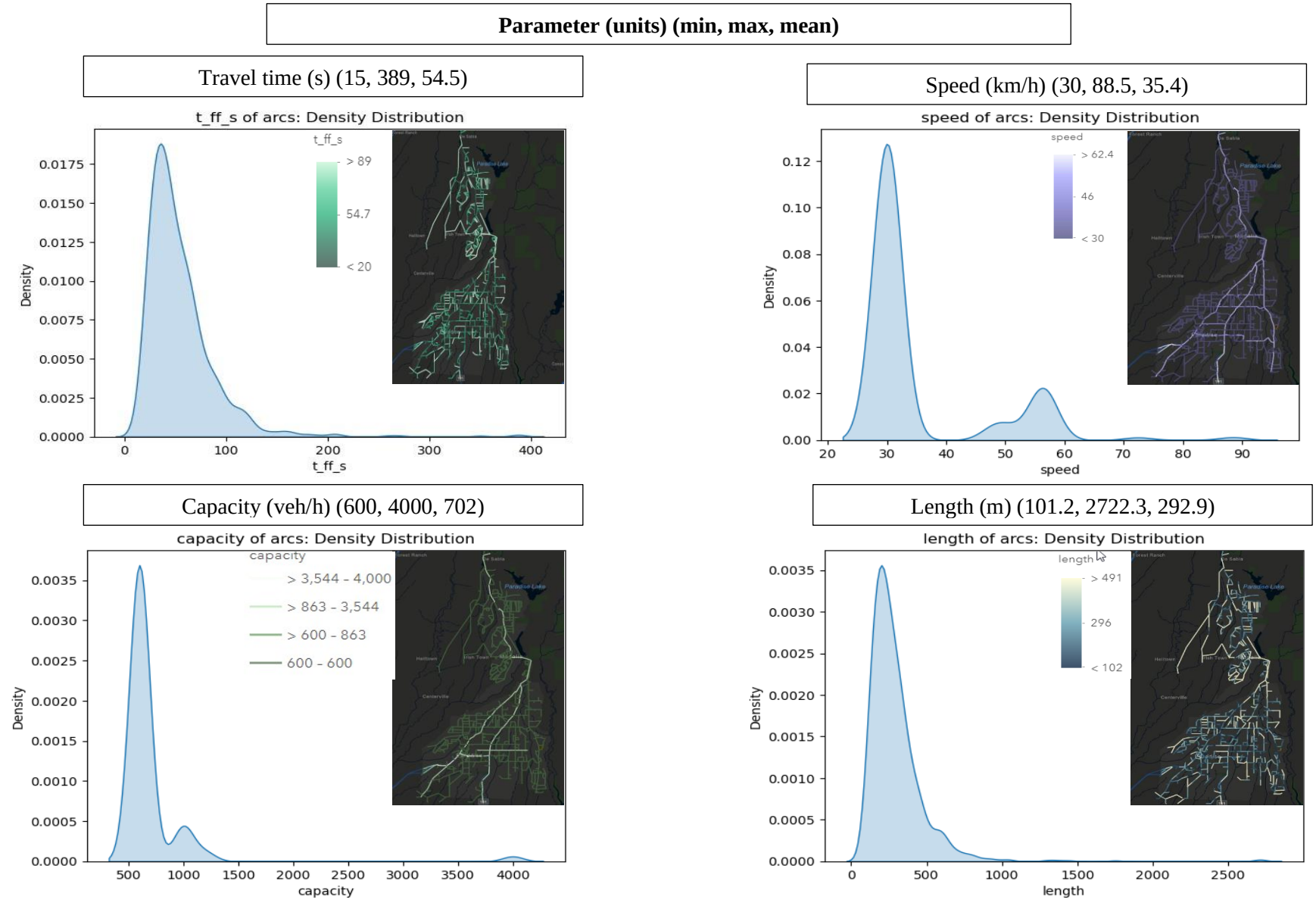

Figure 7 Density distribution of the arcs of the road network, including length, capacity, speed, and travel time

The speed information not available in OSM was completed with the information given by [29], resulting in speeds ranging from 30 to 88.5 km/h. In this study, the authors used a congestion factor obtained from [29] to reduce the speed as an approximation of congestion speed in each arc of the road network. In this case, the minimum travel time is 15 seconds, while the maximum is 389 seconds, determined by the speeds, arc lengths, and congestion factors. The minimum travel time is crucial in the ENP model because it is the foundation for transforming (expanding) the road network for mathematical modeling.

Stage 2: Evacuation with no paths (ENP)

The ENP model requires expanding the road network, resulting in a time-expanded network with 6,673 nodes and 7,834 arcs. The authors initiated the modeling with a large value of T, specifically 1,000 time-units (TUs), where each TU represents 15 seconds. The objective of the ENP model is to maximize the number of vehicles reaching the SN at the minimum time. When constructing the ENP model in our case study, the last time window where all vehicles reached the SN (assumed safe destination), is 411 TU (6165 seconds, 102.75 minutes, or 1 hour and 42 minutes). Figure 8 shows the evacuation rate and % of evacuated vehicles by time in minutes during the planning period of 411 UT (102 minutes).

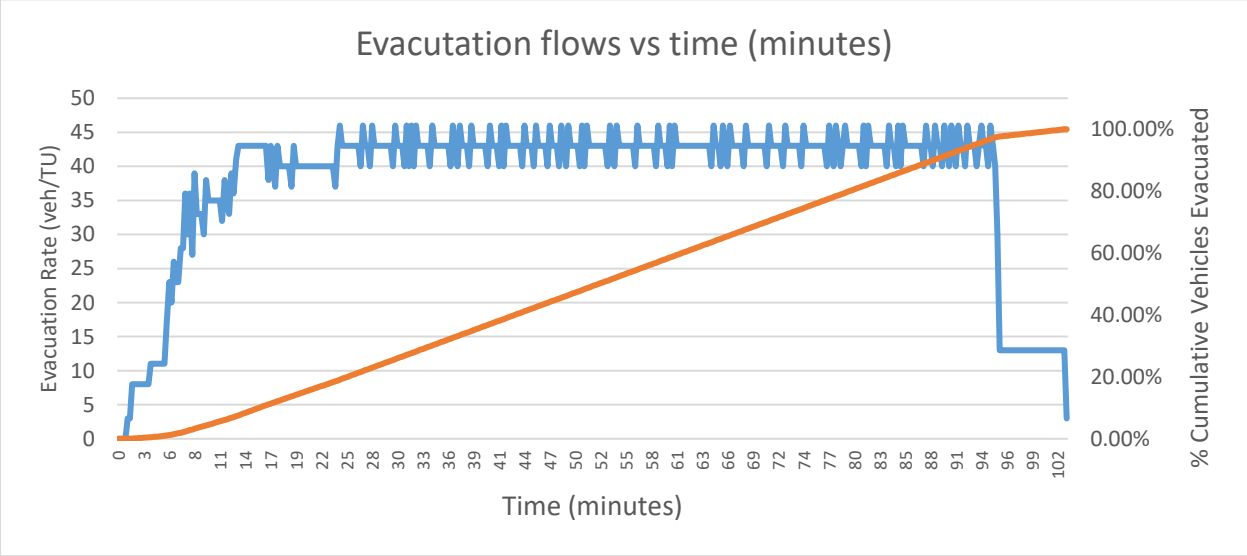

Figure 8 Evacuation percentage with time in minutes

Stage 3: Generation of a pool of paths

The Paradise-Magalia case has 36 source nodes and nine sink nodes (See Figure 6), meaning at least 333 (36*9=333) paths exist. However, the authors included 43 additional feasible paths with a travel time at most double the shortest path of each OD pair, resulting in 376 different paths.

Stage 4: Evacuation plan with paths

To solve the EPWP model, the authors start solving the model with a T = CT obtained in the ENP model (411 TU). However, after iteratively increasing the value of T by one unit, the first feasible solution is obtained when T is equal to 450 TU (equivalent to 6750 seconds, 112.5 minutes, or one hour and 52.5 minutes). This indicates that with the selected set of paths, it is possible to evacuate the city in only ten minutes more than the ENP, where all vehicles use any possible arc in the road network without any pre-existing path set. Figure 9.a depicts that the results of EPWP and ENP models are similar regarding the number of vehicles evacuating on each exit node. Figure 9.b shows differences in the evacuation rate between both models: 30-40 for the EPWP model and 40-45 for the ENP model. Figure 9.c shows differences in the slopes between both models.

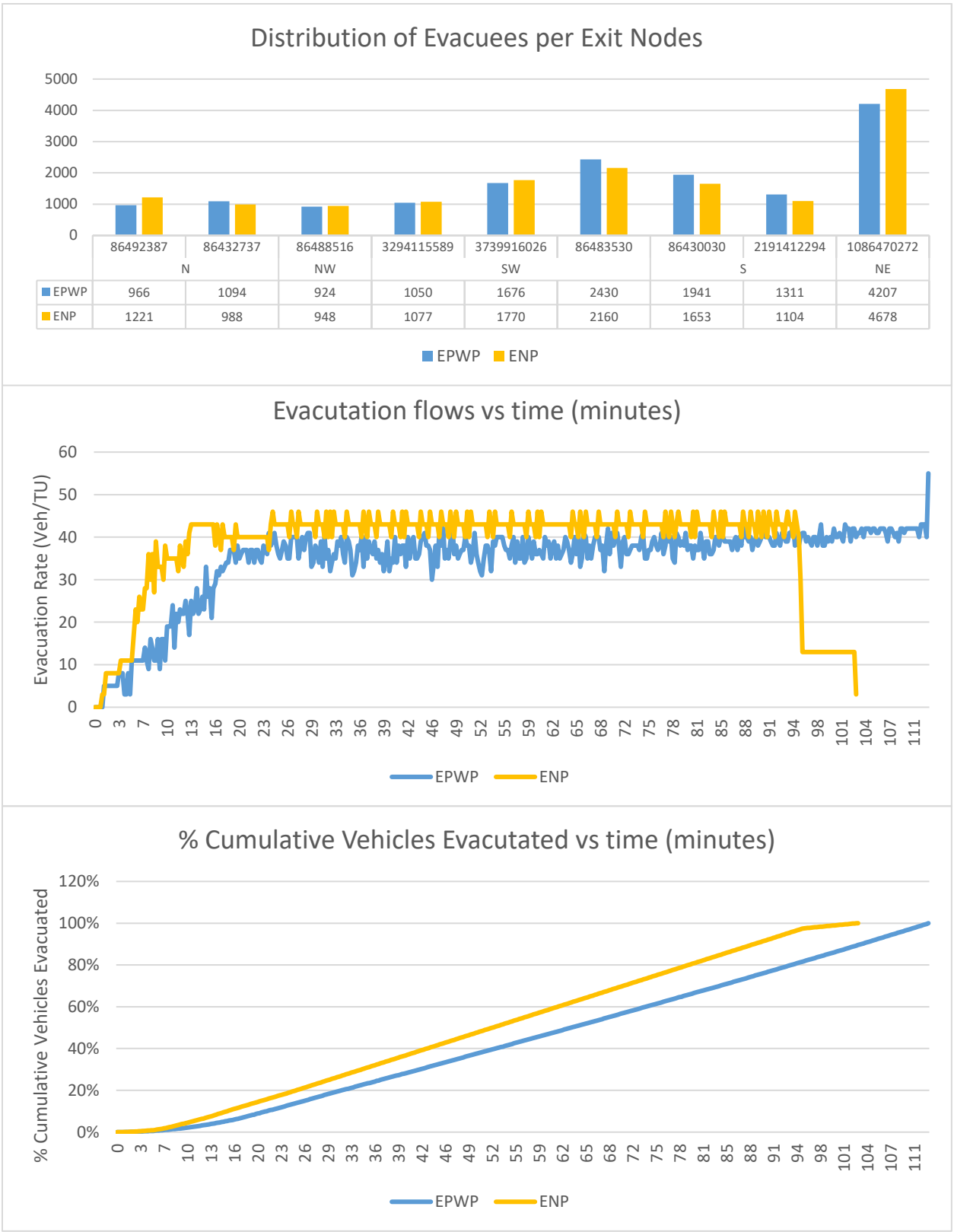

Figure 9 Exit nodes evacuation, evacuation rate, and cumulative percentage of vehicles evacuated under the ENP and EPWP models

The box plot in Figure 10 illustrates the departure and arrival times distribution for vehicles across different paths originating from each census block group (CBG). Figure 10.a shows that most paths have at least one vehicle departing at time zero, while Figure 10.b shows that most paths have at least one vehicle reaching the safe node at time 450. However, the distribution of vehicles throughout the planning horizon varies significantly across different origins.

To understand the behavior of arrival and departure times, we analyzed their correlation against the travel time of paths originating from each CBG, the population of the CBG, and the Social Vulnerability Index (SVI) of each CBG, which depends on socioeconomic characteristics. In this analysis, Figure 11 demonstrates that travel time is the most significant factor in the decision-making process. For those vehicles that depart 50-75% later than the rest of the vehicles, longer travel times tend to result in earlier departures than the rest. Travel times are primarily impacted by the arrival times of vehicles that reach the safe node early. However, this does not significantly alter the arrival times of the remaining vehicles. Note that the population and Social Vulnerability Index were considered in the analysis but did not significantly impact the scheduling of departure and arrival times compared to travel time. Thus, it is possible to indicate that travel time is the primary factor guiding the scheduling of vehicle departures and arrivals. Larger travel times necessitate earlier departures to ensure timely arrivals at safe nodes, highlighting the importance of accounting for travel time in evacuation planning.

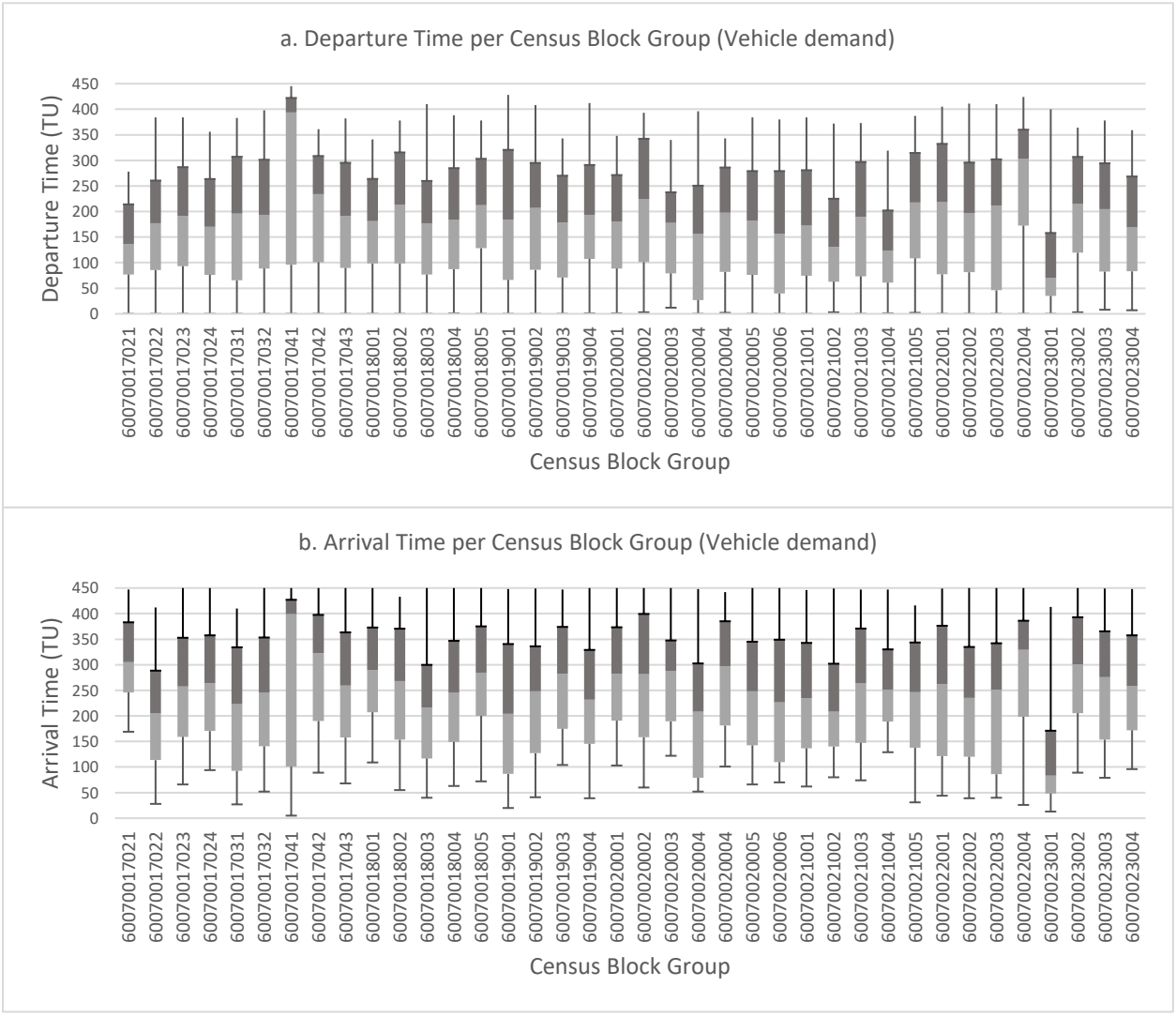

Figure 10 Departure (top) /Arrival (bottom) time comparison between paths

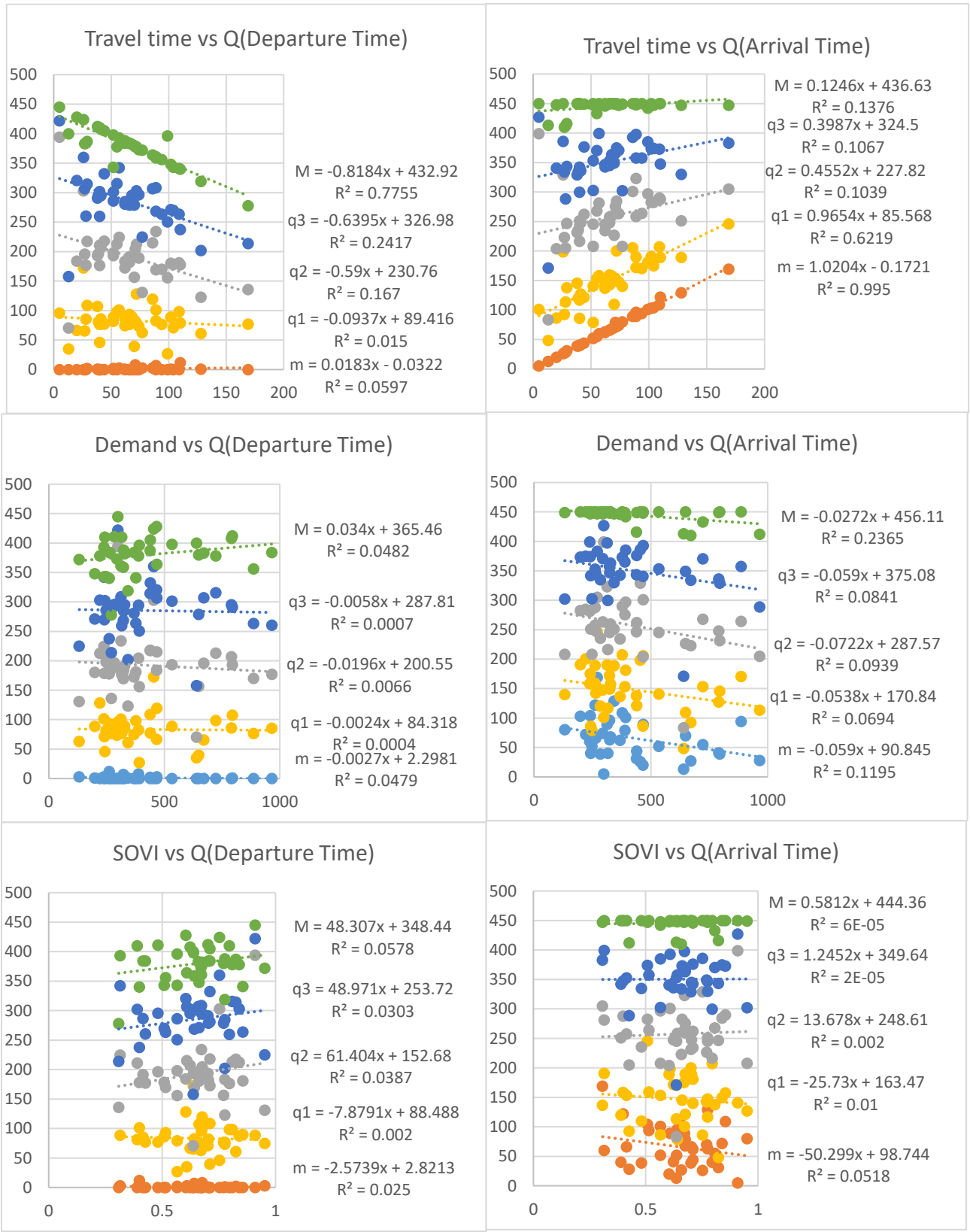

Figure 11 Correlation analysis Travel time OD, demand, and SOVI versus departure and arrival time (Y= Q (Departure/Arrival time) (min, Q1, Q2, Q3, Max))

Figure 12 provides a picture of the evolution of Paradise-Magalia evacuation based on the EPWP model for around 110 minutes, highlighting the minimum number of corridors expected to be used during the evacuation process.

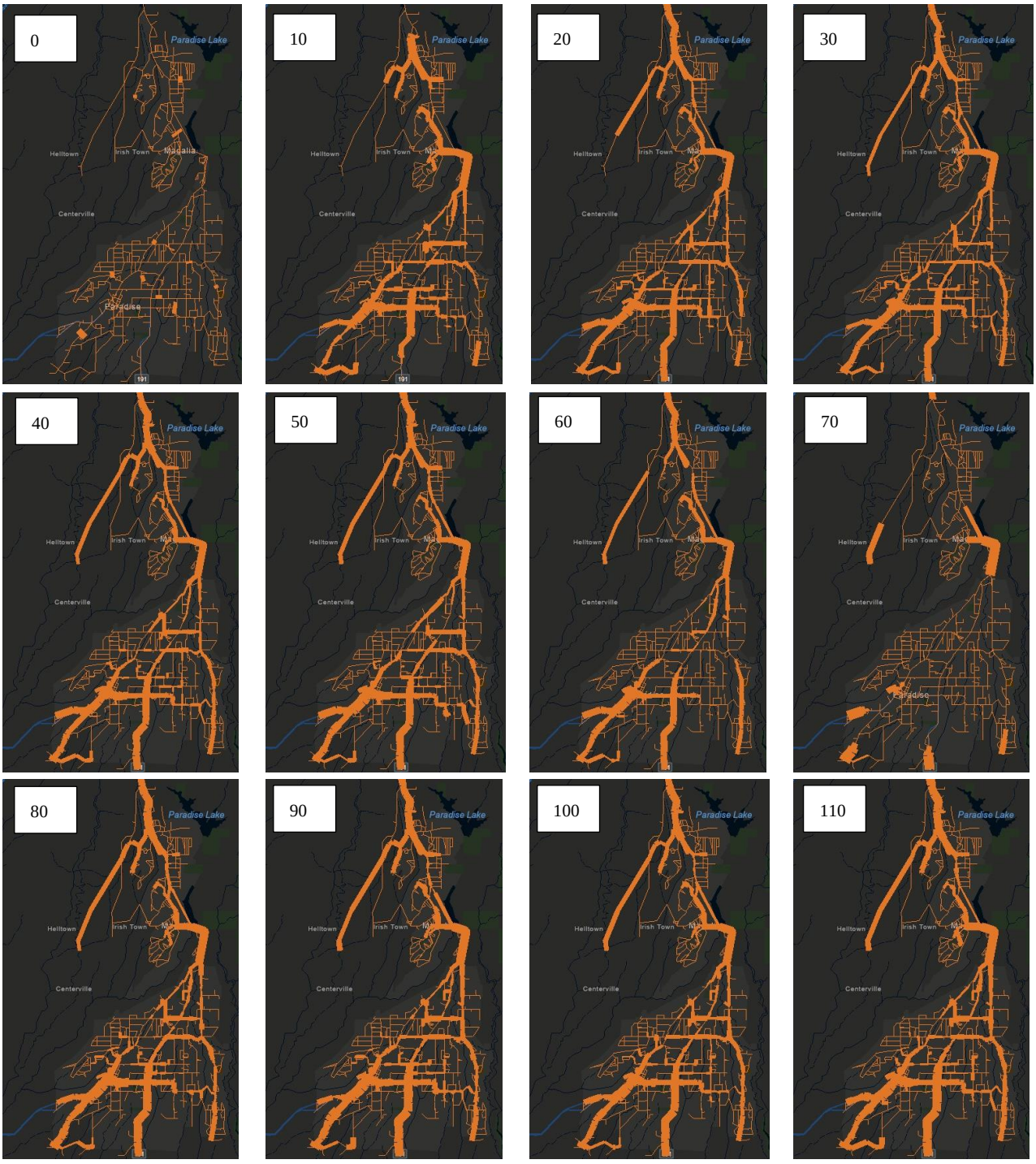

Figure 12 Evolution of the total evacuation on the Paradise-Magalia Case (minutes)

Stage 5: Evacuation Plan Risk Assessment

The authors followed the methodology in [31] to obtain the values of the natural hazard risk at the node level v_j for each node of the road network. Figure 13 provides an overview of the density distribution of

the factors affecting the RNP risk at the local level, particularly for all the road network nodes. Note that the Hansen Accessibility Index (b) displays an almost symmetric distribution, while the Betweenness Centrality (d) among the nodes is skewed to the right. The NRI (c) shows a distribution with three modes. When analyzing the RNP at the local or node level v_j, it has a right-skewed distribution, indicating that some nodes have higher RNP risk than others. The RNP risk at the regional level shows that the RNP risk is higher in the northeast direction; however, there are some smaller peaks of risk in the north, east, and southwest of Paradise and Magalia.

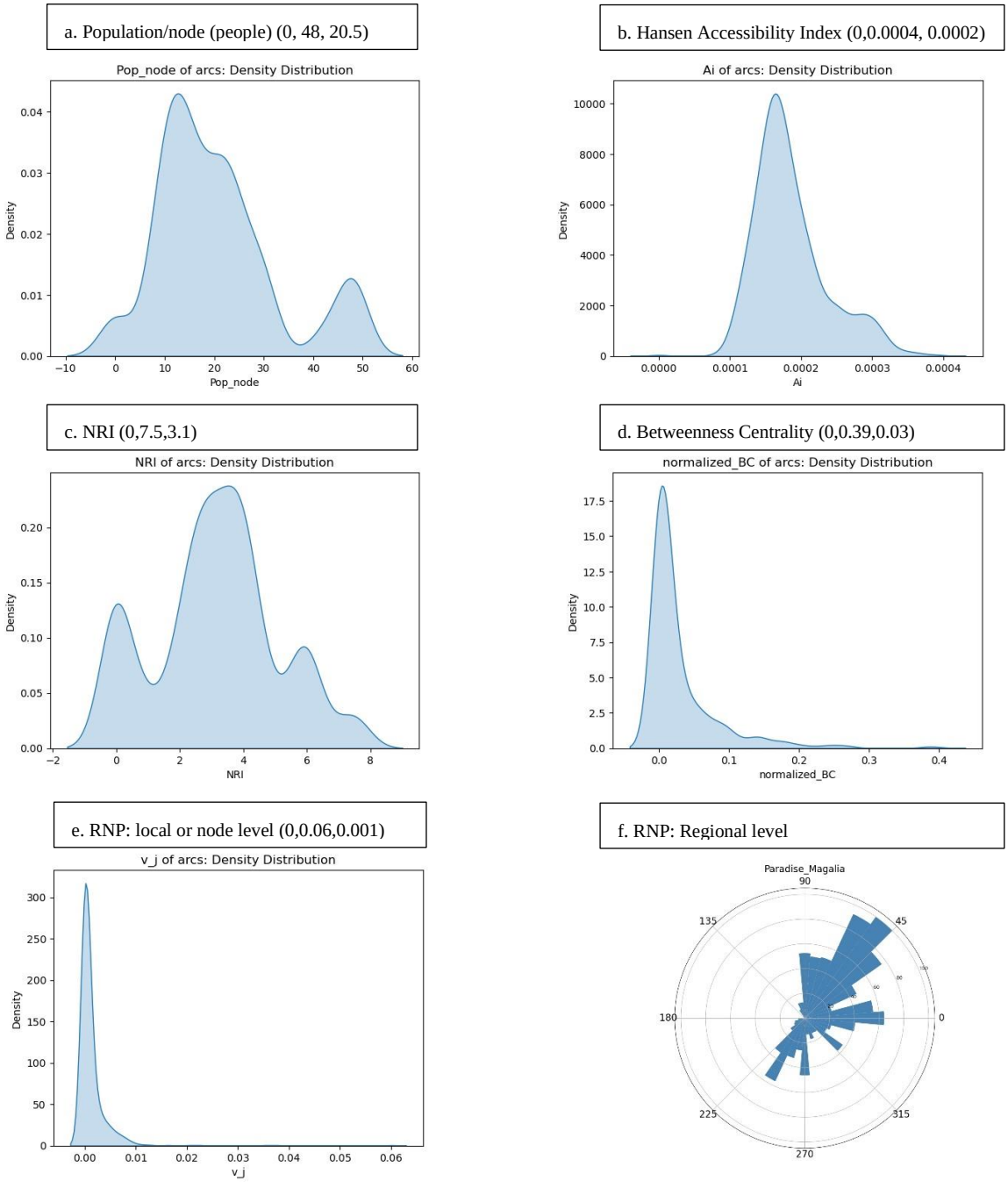

Figure 13 Density probability factors of the v_j parameter (units) (min, max, mean)

This stage considered three different scenarios. First, we modify the pool of paths by using two alternative objective functions in the GPP model. Second, we identify the expected impact of a wildfire on the evacuation by affecting the exit routes in different directions of the road network, such as N, S, W, E, NE, NW, SE, and SW. The RNP risk at the regional level allows for the identification of the probability of wildfire and the estimation of the expected evacuation time under risk conditions. Third, we identify how a real-life wildfire affects the evacuees during the current evacuation plan.

Modifying paths pool: based on different objective functions in the GPP model

First, the authors obtain the pool of paths by using two alternative objectives to the GPP model (see Eq. 25 and Eq. 26). The pool size minimizing time, risk, and risk & time are 362, 356, and 407, respectively. Recall that the risk for each arc is obtained based on Eq. 27, where v_j is the RNP at the node level.

$$r_{ij} = \frac{v_i + v_j}{2} \qquad Eq.27$$

Figure 14 shows that the result of the EPWP model is consistent with their objective. For instance, the model EPWP (r) has the lowest expected evacuation risk perceived by the evacuees, while the model EPWP (r*t) has the lowest expected evacuation risk combined with time. The original model minimizes the time and has the largest expected evacuation risk. Considering the average evacuation time of the ENP model, the EPWP models that minimize evacuation time, risk and risk & time add approximately 10-, 20- and 30-minute delays in the average evacuation time, respectively.

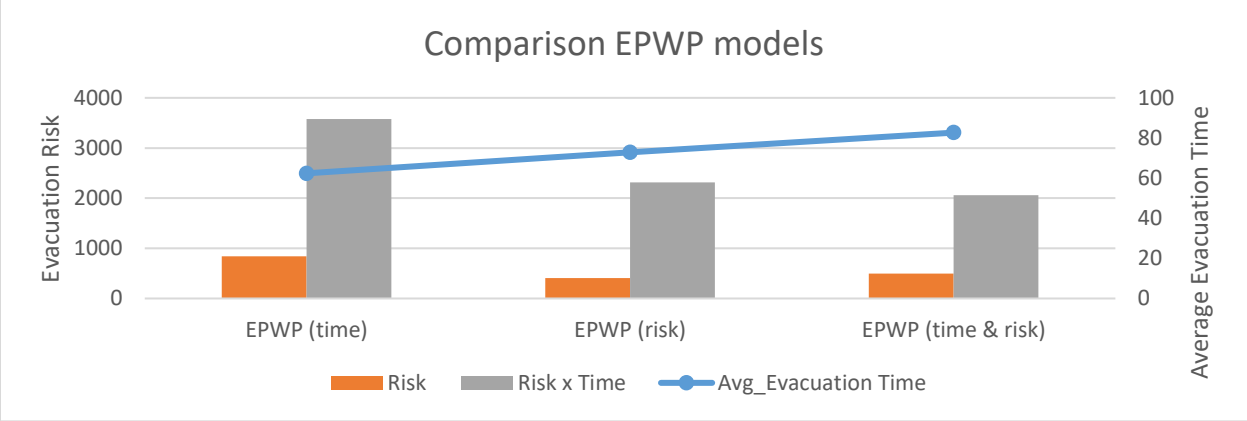

Figure 14 Risk, risk and time, clearance time of EPWP models with different pools of paths.

On the other hand, Figure 15.a shows the difference in the number of vehicles leaving each exit node depending on the model used. Usually, the number of vehicles leaving each exit node is slightly different when using the EPWP model with the pool of paths that minimize time, risk, and risk & time. Figure 15.b and c. show that the average evacuation rate and cumulative are ordered as ENP, EPWP (t), EPWP (r), and EPWP (r*t), respectively. This behavior increases the clearance time, total evacuation time, and average evacuation time of the vehicles. Time and risk are inversely proportional because evacuation time increases when minimizing the expected risk, and vice versa. Therefore, planners need to identify which objective is better for evacuation. For example, a reduction of around 50% in risk implies an increase in clearance time of around 20 to 40 minutes, while the average evacuation time increases by 10 to 20 minutes. Additionally, Figure 16 shows the use of the arcs in the road network in terms of flows during the evacuation process, revealing different behaviors among the various models and objectives. Note that the ENP model utilizes most of the arcs of the road network, while the EPWP models change their patterns depending on the objectives. In this context, the authors identified a measure of importance for each arc (a) on the road network in Eq. 30, based on the average flows (Eq. 28) and their standard deviation (Eq. 29), across the flows obtained in the three scenarios used in the EPWP model: i) time, ii) risk, and iii) time & risk.

$$\bar{F}_a = avg(F_a(EPWP(time)), F_a(EPWP(risk)), F_a(EPWP(time\&risk))) \qquad \text{Eq.28}$$

$$sd(F_a) = sd(F_a(EPWP(time)), F_a(EPWP(risk)), F_a(EPWP(time\&risk))) \qquad \text{Eq.29}$$

$$Importance_a = \bar{F}_a / sd(F_a) \quad \text{Eq.30}$$

The importance $Importance_a$ is greater if the arc has a large average flow and a low standard deviation, meaning that the arc is mostly used independently of the evacuation scenario, with low variability among those scenarios. Figure 16 shows the importance map, highlighting corridors that are vital during evacuation processes, regardless of the scenario under consideration.

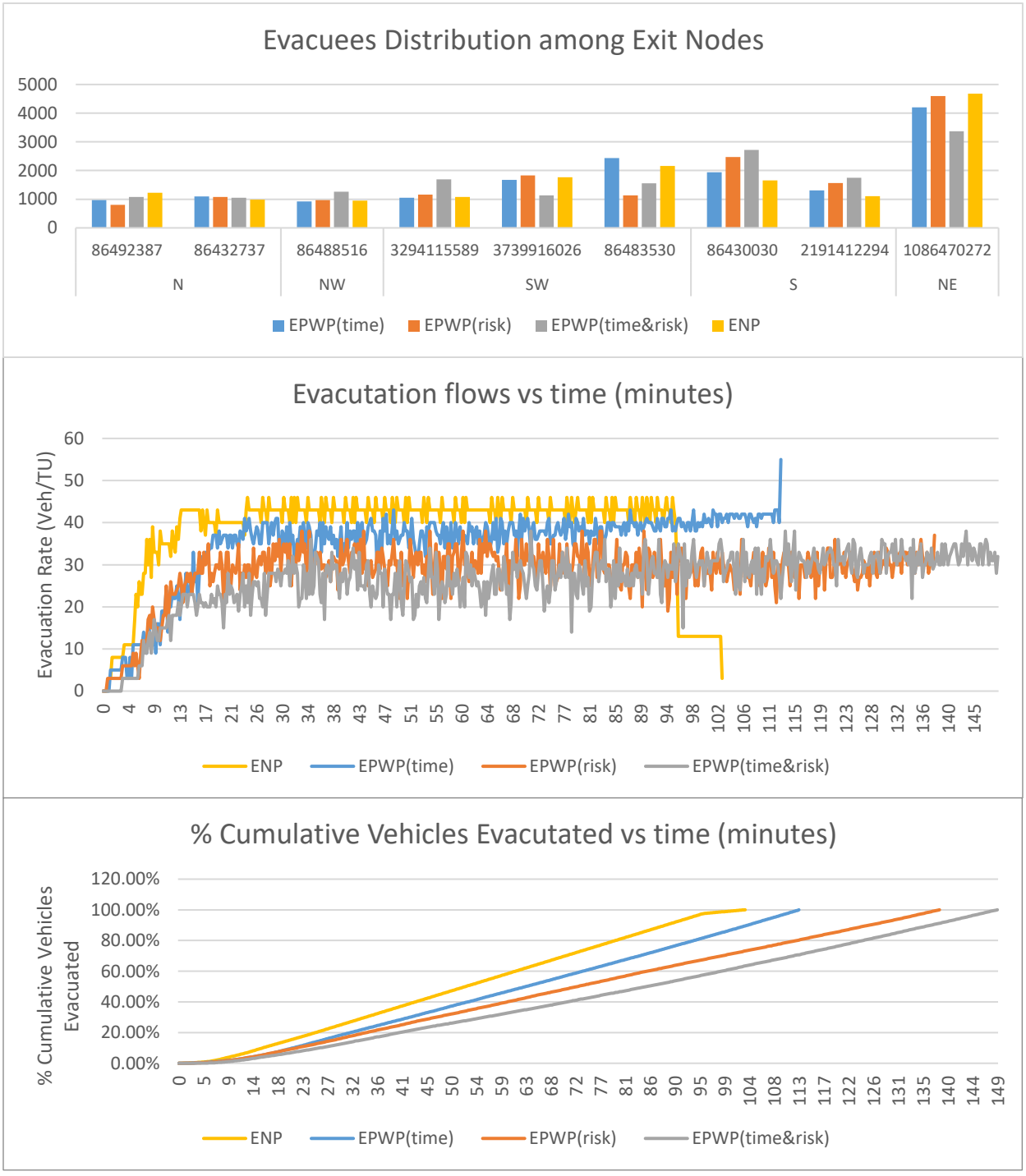

Figure 15 a) distribution of evacuation by exit nodes, b) evacuation flow, and c) cumulative flow of the four model ENP, EPWP (time), EPWP (risk), and EPWP (time & risk)

ENP

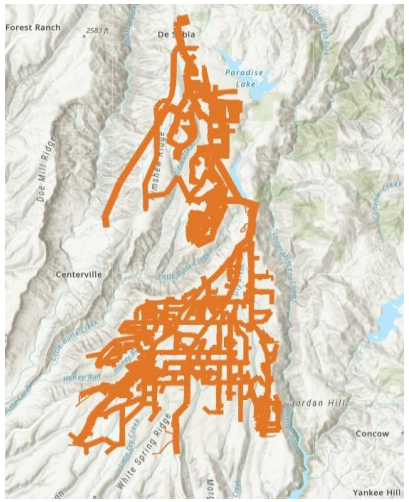

Importance

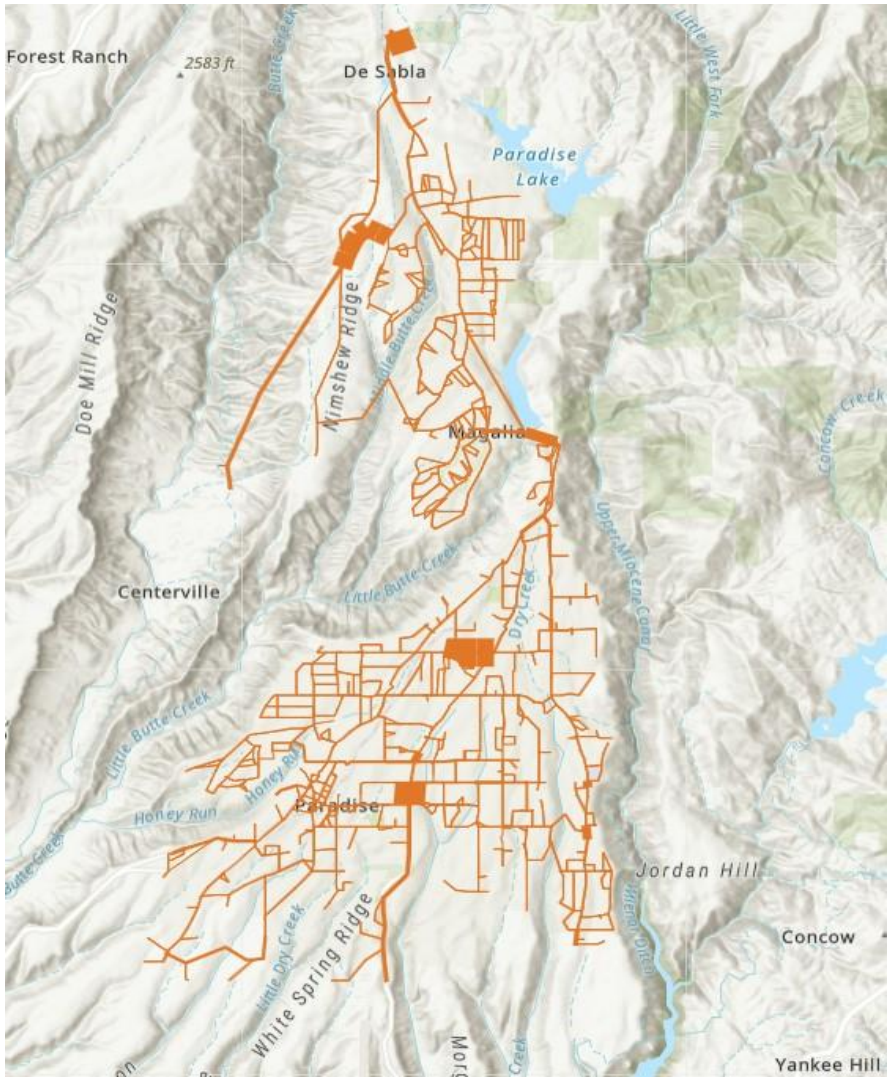

EPWP (Risk)

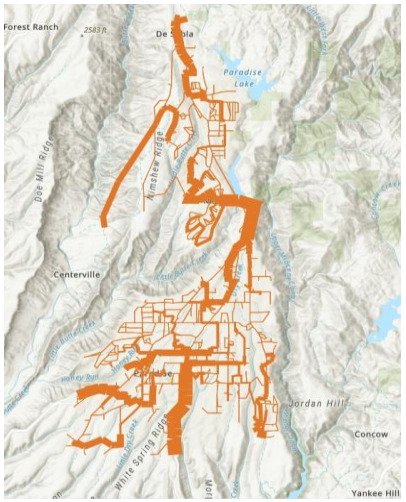

EPWP (Time)

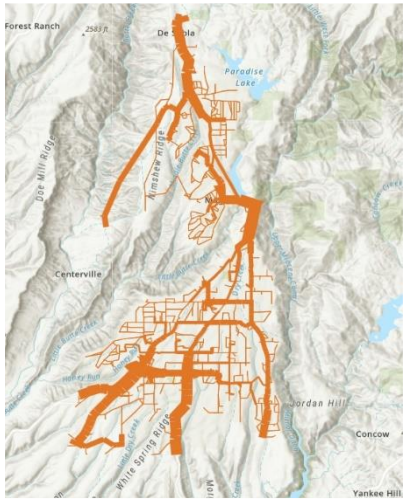

EPWP (Time & Risk)

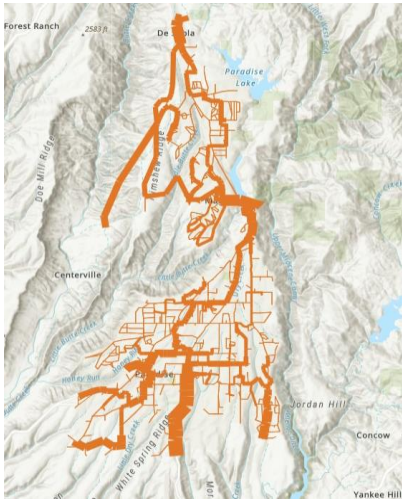

Figure 16 Corridor importance different EPWP objectives

Impact of exit node availability on evacuation performance

Let us assume that the route leading to the closed exit node is blocked, and no vehicles can reach a safe destination through this node. Figure 17 shows the clearance time and average evacuation time when each exit node is closed (independently) using the ENP model. For instance, when node '1086470272' in the NE is closed, the clearance time (CT) increases to 162.5 minutes and the average evacuation time to 72 minutes, compared to the base scenario (102.5 and 52.1 minutes, respectively). This represents a 60% and 38% increase, respectively. In other cases, closing different exit nodes results in evacuation times ranging from 3% to 23% above the base case, while the average evacuation time ranges from 2% to 15% above the base case.

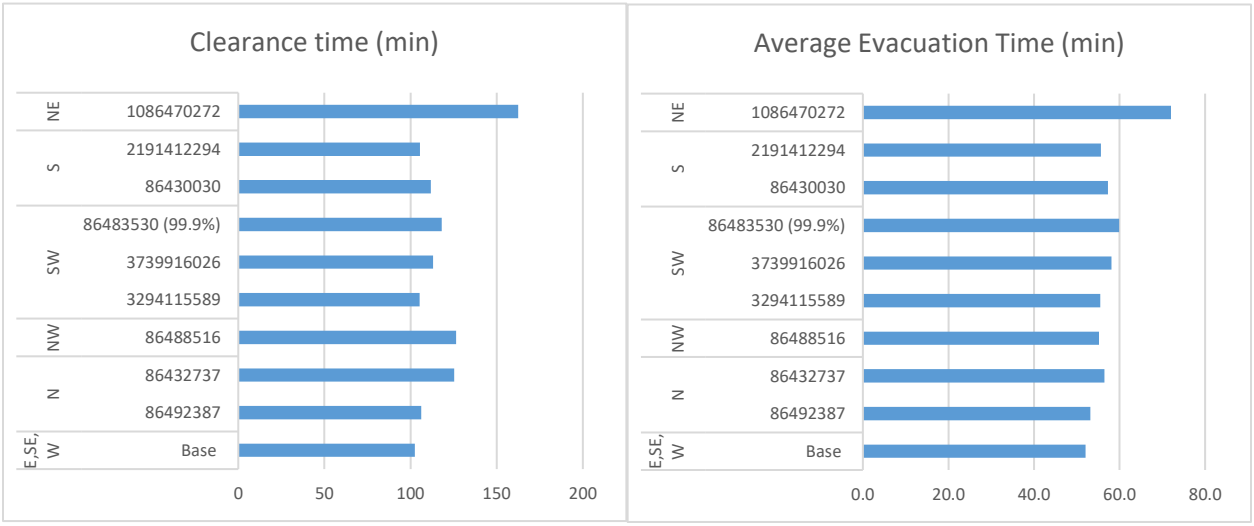

Figure 17 Clearance Time and Average Evacuation Time when closing each exit node

To estimate the probability of affecting any of the eight different directions: d={N, S, W, E, NE, SE, NW, SW} due to the wildfire. The authors use the $\psi_r^{z=wfir}$, this is the *RNP* risk at the regional level r={0, 10, 20,…, 340, 350} depicted in Figure 13.f. Then, the eight directions are subsets of the region; for instance, if r is equal to {0, 10, 20, 340, and 350}, those values represent the East (E), and if r is equal to {30, 40, 50, 60}, then North-East (NE), and so on. The authors use Eq.31 and Eq.32 to estimate the probability of each region (r) and direction (d). On the other hand, Eq.33 allows us to estimate the expected clearance time (CT), total evacuation time (TET), and average evacuation (avg_ET) of each direction.

$$p(x = r) = \frac{\psi_r^{z=wfir}}{\sum_r \psi_r^{z=wfir}} \qquad \textit{Eq.31}$$

$$p(x = r|\, y = d) = \frac{\psi_r^{z=wfir}}{\sum_{r \epsilon d} \psi_r^{z=wfir}} \qquad \textit{Eq.32}$$

$$E[Var_d] = \sum_{r\,\epsilon\,d} p(x = r|\, y = d) * Var_r \qquad \textit{Eq.33}$$

Eq.30 is the sum of the multiplication between the variable's value (CT, TET, avg_ET) when the natural hazard blocks the exit in the region r times the probability of this hazard in the region r belonging to the directions d. For example, note that in the NE direction, the exit node '1086470272' is located in the region of 50°. The consequence of closing this exit node is a clearance time of 650 Units of Time (U.T.) (2 hours and 42 minutes). In contrast, if the wildfire affects other regions (r) like 30°,40°, or 60° in this direction (d), there is no node affected, and the CT is the same as the *base case*, which is 410 U.T. (1 hour and 42 minutes). Therefore, the expected clearance time if a wildfire threatens the northeast side of the road network is around 486 U.T. (around 2 hours) (see Eq.34 and Eq.35).

$$E[CT_{NE}] = p(x = 50|\, y = NE) * CT_{50} + \big(1 - p(x = 50|\, y = NE)\big) * CT_{base} \qquad \text{Eq.34}$$

$$E[CT_{NE}] = 0.32 * 650 + (0.68) * 410 = 486 \quad \text{Eq.35}$$

Figure 18 provides the steps to estimate the expected CT, TET, and avg_ET for the eight directions. The expected CT under wildfire threat on all cardinal directions independently is 442 UT (110 minutes or 1 hour and 50 minutes), TET is 3438858 UT (or 859,714 minutes), and avg_ET is 55.1 minutes.

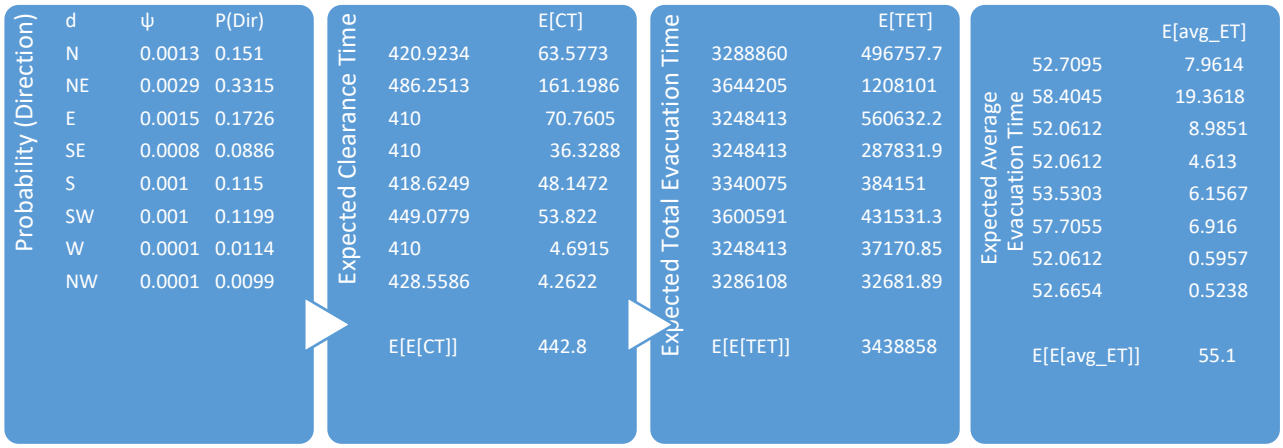

Figure 18 Estimation of expected clearance time, total evacuation time, and average evacuation time

Analyzing the risk with a real case scenario with the Camp Fire in Paradise

To identify the performance of the evacuation during a real-life wildfire, the authors estimate the number of affected vehicles in the road network depending on the start of the evacuation in contrast with the start of the wildfire event. In this case, the real-life wildfire event is the Camp Fire, obtained from Szasdi-Bardales et al. [33]. First, the authors identify the timeframe when the Camp Fire affected each arc of the road network. For instance, note in Figure 19 that no arc is affected by the wildfire at time 0 (3:30 p.m. 11/08/2018). Only after 70 minutes (4:40 p.m. 11/08/2018) does the wildfire impact the first node. Also, 600 minutes after the beginning of the Camp Fire, 75% of the arcs of the road network in Magalia (North) and Paradise (South) are affected by the wildfire, specifically those in Paradise. Figure 20 shows a sensitivity analysis of the number of affected vehicles based on the starting time of the evacuation after the beginning of the wildfire. For instance, if the evacuation starts at the same time as the beginning of the fire, it is possible that after 70 minutes (4,200 seconds or 280 U.T.), vehicles could be affected on the road network if not evacuated; however, they could reach a safe destination before the fire blocks the exit routes.

When analyzing the number of vehicles affected due to exit nodes potentially being blocked, note in Figure 20 that there are no affected vehicles at the exit nodes when the evacuation starts within 117 minutes. However, when the delay is between 117 and 227 minutes, around 53 vehicles are affected per minute. At 227 minutes, 5,782 (37%) of affected vehicles are expected to be impacted when exiting the city, and this value remains steady for around 50 minutes. Note also that if the evacuation starts 552 minutes after the beginning of the wildfire, around 80% of the total demand of vehicles (12,442) will be trapped at the exit nodes of the road network.

On the other hand, when analyzing the vehicles affected in the road network over time, we observe a similar pattern to the expected vehicles blocked at the exit nodes, with slight differences. For instance, the number of vehicles affected in the road network is greater than zero, even when the evacuation starts 7 minutes after the wildfire is noticed. This number of affected vehicles in the road network increases steadily over time. Still, it remains constant between 250 and 350 minutes before growing again until it reaches 12,082 vehicles, the maximum number of vehicles that could be affected in the road network due to the wildfire.

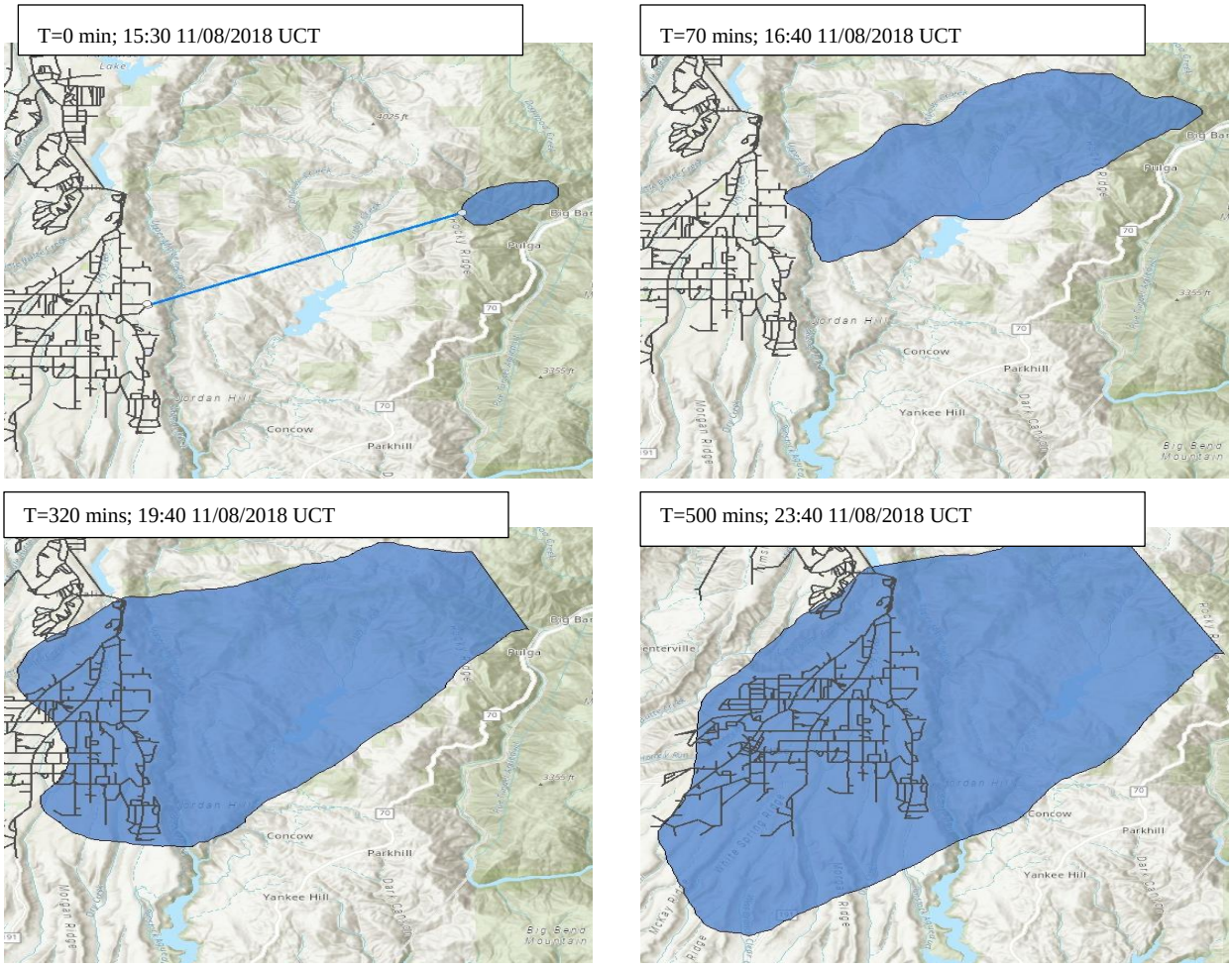

Figure 19 Sample of simulation of the Camp fire perimeters obtained from Szasdi-Bardales, et al., [35]

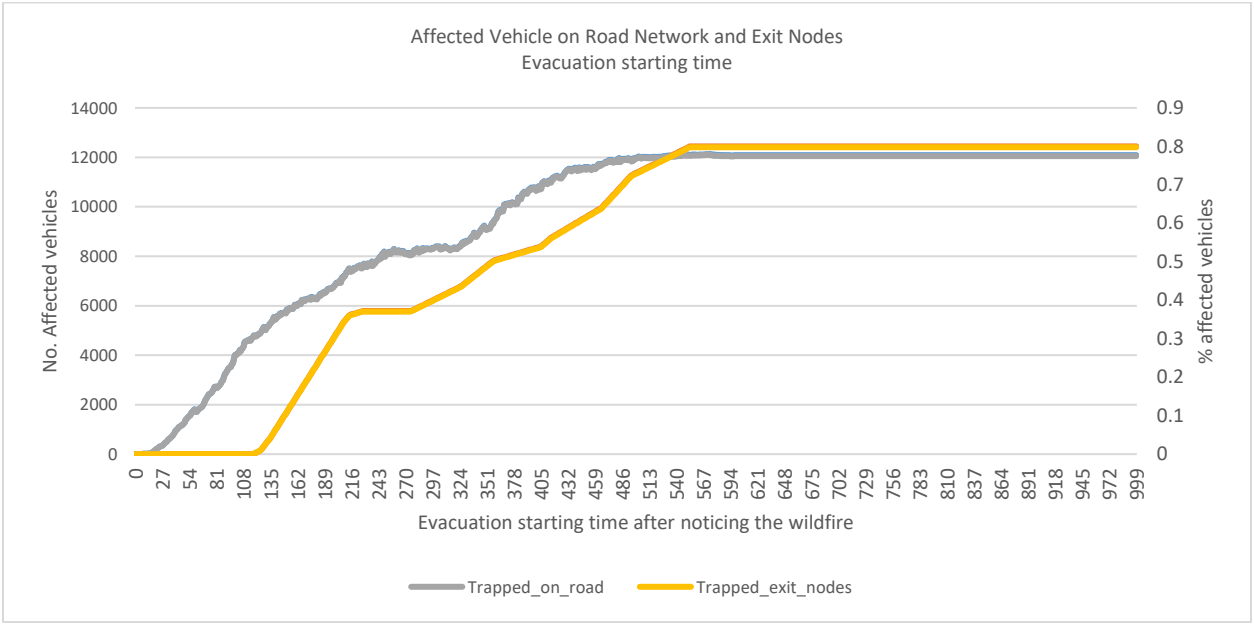

Figure 20 Number of vehicles affected vs the starting time of the evacuation

KEY FINDINGS AND CONCLUSIONS

This paper provided a methodology to identify evacuation plans for no-notice wildfire events. Six main tasks were completed using the American Community Survey, OpenStreetMap, NRI datasets, and the RNP risk at different levels of the road network [31]. In this paper, the authors estimated the minimum clearance time, a pool of paths between each OD pair, the minimum number of paths that could be used to evacuate the population in the minimum time, the RNP risk at the node and arc level, and regional. The authors also analyzed the sensitivity of the evacuation performance based on different objective functions and closures of exit routes. The authors also evaluated how the evacuation plans were performed during a simulated wildfire event in Paradise, California.

When constructing and loading the road network, it is important to note that the minimum travel time on all arcs determines the model's complexity. Therefore, it is crucial to identify the best tolerance to use when simplifying the network without losing its structure. Additionally, the ENP model does not provide a plan for the evacuation process. However, it is possible to obtain an evacuation plan when combined with the GPP model into the EPWP model. Additionally, modifying the objective of the pool of paths on the GPP model has impacts the objectives of the EPWP model, as well as closing each exit route has also an impact on the evacuation process on the ENP model.

In general, the travel time from origin to destination for each path is the primary factor guiding the scheduling of vehicle departures and arrivals. However, with the evacuation plan risk assessment that considers the inclusion of a different pool of paths that minimize the total risk between each origin-destination (OD) pair, in addition to those that minimize time, it becomes possible to identify the minimum number of corridors vital for evacuation planning. Additionally, it is possible to identify the most critical exit routes, directions with higher risk, and the expected evacuation time under wildfire risk.

Finally, testing the evacuation plan against the simulation of the Camp Fire shows that even in the most idealistic scenario, when the evacuation starts with the fire 9 km away from the city, there is a risk of people being trapped in the road network. If evacuation orders do not start within approximately 2 hours, the consequences increase substantially regarding the risk of being trapped. This case study demonstrates the need to develop strategies to alleviate such situations and avoid large-scale calamities in the event of a no-notice wildfire when the city's current capacity does not allow demand to evacuate effectively.

ACKNOWLEDGEMENTS

This study was partially funded by a California Department of Transportation grant through the National Center for Sustainable Transportation at the University of California, Davis, and NIST.

AUTHOR CONTRIBUTION STATEMENT

The authors confirm their contribution to the paper: study conception, design, methodology, and data identification: MJ and DR; review and data assembly: DR; analyses and interpretation of results: DR, MJ; and draft manuscript preparation: DR, MJ. All authors reviewed the results and approved the final version of the manuscript.

REFERENCES

[1] DHS, "Department Homeland Security," 05 2022. [Online]. Available: https://www.dhs.gov/natural-disasters.

[2] H. Ritchie and M. Roser, "Natural Disasters," *Our world in Data*, 2014.

[3] T. Cova, D. Theobald, J. Norman and L. Siebeneck, "Mapping wildfire evacuation vulnerability in the western US: The limits of infrastructure," *GeoJournal*, vol. 78, p. 273–285, 2013.

[4] S. Wong, J. Broader and S. Shaheen, "Review of California wildfire evacuations from 2017 to 2019," UCITS, 2020.

[5] N. Menon, B. Staes and R. Bertini, "Measuring Transportation Network Performance During Emergency Evacuations: A Case Study of Hurricane Irma and Woolsey Fire.," Arlington TX, 2020.

[6] F. Maltinti, D. Melis and F. Annunziata, "Road network vulnerability: A review of the literature," *ICSDC 2011: Integrating Sustainability Practices in the Construction Industry,* pp. 677-685, 2012.

[7] Climate, "climate.org," 2021. [Online]. Available: https://www.climate.gov/news-features/blogs/beyond-data/2021-us-billion-dollar-weather-and-climate-disasters-historical.

[8] statista, "statista," [Online]. Available: https://www.statista.com/search/?q=Largest+wildfires+in+California&Search=&p=1. [Accessed 22 7 2024].

[9] R. Blanchi, J. Whittaker, K. Haynes, J. Leonard and K. Opie, "Surviving bushfire: the role of shelters and sheltering practices during the Black Saturday bushfires," *Environmental Science & Policy,* vol. 81, pp. 86-94, 2018.

[10] M. Siam, H. Wang, M. Lindell, C. Chen, E. Vlahogianni and K. Axhausen, "An interdisciplinary agent-based multimodal wildfire evacuation model: Critical decisions and life safety," *Transportation research part D: transport and environment,* vol. 103, p. 103147, 2022.

[11] G. Lim, S. Zangeneh, M. Baharnemati and T. Assavapokee, "A capacitated network flow optimization approach for short notice evacuation planning," *European Journal of Operational Research,* vol. 223, no. 1, pp. 234-245, 2012.

[12] N. Altay and W. Green, "Or/ms research in disaster operations management," *European Journal of Operation Research,* vol. 175, no. 1, pp. 475-93, 2006.

[13] E. Maspero and H. Ittmann, "Rise of humanitarian logistics," 2008.

[14] C. Rawls and M. Turnquist, "Pre-positioning of emergency supplies for disaster response," *Transportation research part B: Methodological,* vol. 44, no. 4, pp. 521-534, 2010.

[15] G. Galindo and R. Batta, "Review of recent developments in or/ms research in disaster operations management," *Europen Journal of Operation Research,* vol. 230, no. 2, pp. 201-11, 2013.

[16] G. Galindo and R. Batta, "Prepositioning of supplies in preparation for a hurricane under potential destruction of prepositioned supplies," *Socio-Economic Planning Sciences,* vol. 47, no. 1, pp. 20-37, 2013.

[17] D. Rivera-Royero, G. Galindo and R. Yie-Pinedo, "A dynamic model for disaster response considering prioritized demand points," *Socio-economic planning sciences,* vol. 55, pp. 59-75, 2016.

[18] S. Shahparvari, P. Chhetri, A. Abareshi and B. Abbasi, "Multi-objective decision analytics for short-notice bushfire evacuation: an Australian case study," *Australasian Journal of Information Systems,* 2015.

[19] B. Zhao and S. Wong, "Developing transportation response strategies for wildfire evacuations via an empirically supported traffic simulation of Berkeley, California.," *Transportation research record,* vol. 2675, no. 12, pp. 557-582, 2021.

[20] T. Cova, P. Dennison and F. Drews, "Modeling evacuate versus shelter-in-place decisions in wildfires.," *Sustainability,* vol. 3, no. 10, pp. 1662-1687, 2011.

[21] S. Grajdura, X. Qian and D. Niemeier, "Awareness, departure, and preparation time in no-notice wildfire evacuations," *Safety science,* vol. 139, p. 105258, 2021.

[22] V. Bayram, "Optimization models for large scale network evacuation planning and management: A literature review," *Surveys in Operations Research and Management Science,* vol. 21, no. 2, pp. 63-84, 2016.

[23] P. Murray-Tuite and B. Wolshon, "Evacuation transportation modeling: An overview of research, development, and practice," *Transportation Research Part C: Emerging Technologies,*, vol. 27, pp. 25-45, 2013.

[24] Q. Lu, B. George and S. Shekhar, "Capacity constrained routing algorithms for evacuation planning: A summary of results," in *In International symposium on spatial and temporal databases* , Berlin, Heidelberg, 2005.

[25] M. Osman and B. Ram, "Evacuation route scheduling using discrete time-based capacity-constrained model," in *IEEE International Conference on Industrial Engineering and Engineering Management*, 2011 .

[26] M. Rungta, G. Lim and M. Baharnemati, "Optimal egress time calculation and path generation for large evacuation networks," *Annals of Operations Research,* vol. 201, no. 1, pp. 403-421, 2012.

[27] H. Zheng, Y. Chiu, P. Mirchandani and M. Hickman, "Modeling of evacuation and background traffic for optimal zone-based vehicle evacuation strategy," *Transportation Research Record,* vol. 2196, no. 1, pp. 65-74, 2010.

[28] G. Boeing, "OSMnx: New Methods for Acquiring, Constructing, Analyzing, and Visualizing Complex Street Networks," *Computers, Environment and Urban Systems,* vol. 65, pp. 126-139, 2017.

[29] M. Zilske, A. Neumann and K. Nagel, "OpenStreetMap for traffic simulation," 2011.

[30] U.S. Census Bureau, "American Community Survey 3-year Public Use," U.S. Census Bureau, 2020.

[31] D. Rivera-Royero and M. Jaller, "A Methodology for Assessing the Road Network Risk Performance Employing a Standardized Spatial Risk Analysis," 2024.

[32] Federal Emergency Management Agency , "National Risk Index (Technical Documentation) v 1.19," FEMA, 2023.

[33] F. Szasdi-Bardales, K. Shamsaei, N. Lareau, T. Juliano, B. Kosovic, H. Ebrahimian and N. Elhami-Khorasani, "Integrating dynamic wildland fire position input with a community fire spread simulation: A case study of the 2018 Camp Fire," *Fire Safety Journal,* vol. 143, p. 104076, 2024.

[34] H. Sbayti and H. Mahmassani, "Optimal scheduling of evacuation operations," *Transportation Research Record,* vol. 1964 , no. 1, pp. 238-246, 2006.

[35] Y. Chiu and H. Zheng, "Real-time mobilization decisions for multi-priority emergency response resources and evacuation groups: model formulation and solution," *Transportation Research Part E: Logistics and Transportation Review,* vol. 43, no. 6, pp. 710-736, 2007.

[36] Y. Chiu, H. Zheng, J. Villalobos and B. Gautam, "Modeling no-notice mass evacuation using a dynamic traffic flow optimization model," *Transactions,* vol. 39, no. 1, pp. 83-94, 2007.

[37] V. Bayram, B. Tansel and H. Yaman, "Compromising system and user interests in shelter location and evacuation planning," *Transportation research part B: methodological,* vol. 72, pp. 146-163, 2015.

[38] H. Abdelgawad, B. Abdulhai and M. Wahba, "Multiobjective optimization for multimodal evacuation," *Transportation Research Record,* vol. 2196, no. 1, pp. 21-33, 2010.

[39] A. Li, L. Nozick, N. Xu and R. Davidson, "Shelter location and transportation planning under hurricane conditions," *Transportation Research Part E: Logistics and Transportation Review,* vol. 48, no. 4, pp. 715-729, 2012.

[40] H. Tuydes-Yaman and A. Ziliaskopoulos, "Modeling demand management strategies for evacuations," *Annals of Operations Research,* vol. 217, pp. 491-512, 2014.

[41] H. Gan, K. Richter, M. Shi and S. Winter, "Integration of simulation and optimization for evacuation planning," *Simulation Modelling Practice and Theory,,* vol. 67, pp. 59-73, 2016.

[42] X. Chen and F. Zhan, "Agent-based modeling and simulation of urban evacuation: relative effectiveness of simultaneous and staged evacuation strategies," in *Agent-based modeling and simulation*, Palgrave Macmillan, London., 2014, pp. 78-96.

1
2
3